Blind Satellite Inter-Gateway Interference Mitigation

Jesús Arnau and Carlos Mosquera
Signal Theory and Communications Department, University of Vigo - 36310 Vigo, Spain
{suso,mosquera}@gts.uvigo.es

***Abstract*—Broadband multibeam satellites may require very high feeder link bandwidths to relay all the signals to a unique gateway. This is the case if they enforce an aggressive spectrum reuse across all the user beams and the overall capacity increases accordingly. If the processing is split among different gateways, then the inter-gateway interference must be counteracted to provide acceptable quality of service. In this paper, we propose to blindly estimate the covariance matrix of the received signals at each gateway, and then perform minimum mean-squared error combining based on that estimate and on the subset of channel responses that the gateway can get to learn. Results show that, even with no collaboration among the gateways, significant throughput increases are achieved with respect to a traditional scenario with partial frequency reuse, at the cost of degraded availability levels.**

***Index Terms*—Multibeam satellites; multiple gateways; LMMSE receiver; sample matrix inversion; SMI.**

I. Introduction

Today's interactive broadband satellite service is mainly supported by multiple small antenna beams. This allows for better carrier to noise provisioning, but also introduces interference among adjacent beams due to the side lobes of the antenna patterns. In order to cope with the ever-increasing throughput which is demanded by all wireless systems [1], aggressive frequency reuse patterns, together with interference mitigation techniques, have been proposed [2]–[4]. A problem affecting these techniques is that they need to relay all the signals received at the satellite to a single gateway, which may result in a extremely large feeder link bandwidth unavailable in commonly used frequency bands[1]. In consequence, the limited channelization capacity of a unique gateway calls for the use of several gateways, each managing a lower amount of resources. If beams are grouped into clusters, a given gateway per cluster can manage the associated inbound and outbound traffic if the system is properly dimensioned. Note that as long as the resulting gateways are sufficiently separated on Earth, the same feeder link band can be reused in all the corresponding satellite to gateway links. This multi-gateway scheme is not void of problems, since severe inter-cluster interference is still present and needs to be handled by separated gateways, as opposed to the ideal centralized gateway managing all the beams. For the forward link, this fact was shown among others in [8], [9], while the return link was studied in [4], [10]. The latter references showed the benefits of inter-gateway cooperation, when feasible.

In this paper, we will focus on the return link of a transparent geostationary satellite system, and try to mitigate interference effectively without inter-gateway collaboration. We propose to blindly estimate the covariance matrix of the received signals at each gateway, in the fashion of the adaptive beamforming literature. Then, we perform minimum mean-squared error combining based on that estimate, and on the entries of the channel matrix that the gateway knows. Results will show that, even with no collaboration among the gateways, promising throughput increases are possible with respect to a traditional scenario with partial frequency reuse. We will not explore other possible divisions of traffic among gateways, such as the allocation of different portions of spectrum to different gateways, which could potentially avoid the cross-interference of signals going to different gateways, but might find other implementation barriers in terms of management of the network.

The remaining of the paper is structured as follows: Section II details the system model assumed, Section III explains the proposed solution, Section IV shows the simulation results obtained after simulation, Section V sketches some practical limitations affecting the solution, and finally Section VI reports the conclusions of the paper.

II. System model

We consider the return link of a multibeam satellite system with a K-element antenna serving the same number of beams on Earth. At a given time instant, the set of signals received at the satellite is given by

$$\mathbf{y}_{\mathrm{T}} = \mathbf{H}_{\mathrm{T}}\mathbf{s}_{\mathrm{T}} + \mathbf{n}_{\mathrm{T}} \tag{1}$$

where $\mathbf{s}_{\mathrm{T}} \in \mathcal{S}^{K\times 1}$ is the unit-power transmitted signal vector (with $\mathcal{S}$ the set of possible transmitted symbols), $\mathbb{E}\left[\mathbf{s}_{\mathrm{T}}\mathbf{s}_{\mathrm{T}}^{H}\right] = \mathbf{I}$ ($\mathbf{I}$ is the identity matrix and $(\cdot)^H$ denotes the Hermitian transpose), $\mathbf{y}_{\mathrm{T}} \in \mathcal{C}^{K\times 1}$ is the received signal vector at the satellite, $\mathbf{n}_{\mathrm{T}} \sim \mathcal{CN}\left(\mathbf{0}, \sigma^2\mathbf{I}\right)$ is the noise vector, and σ^2 is the

Jesús Arnau is now with the Mathematics and Algorithmic Sciences Lab, France Research Center, Huawei Technologies Co., Ltd (jesus.arnau@huawei.com).

Work partially funded by the Spanish Government under projects COMONSENS (CSD2008-00010) and COMPASS (TEC2013-47020-C2-1-R), by the Galician Regional Government and the European Development Fund under projects "Consolidation of Research Units" (GRC2013/009), REdTEIC (R2014/037) and AtlantTIC, and by the EU 7$^{\mathrm{th}}$ Framework Program under project BATS (contract no. 317533).

[1]Significantly higher bandwidths come from the allocation of higher frequency bands such as Q or V, an even above, to the feeder link. However, atmospheric attenuation is more severe in those bands [5]. This, together with the need for high feeder link availability, would require the deployment of redundant gateways (see [6], [7] and references therein), limiting the potential benefits.

noise power. The channel matrix $\mathbf{H}_{\mathrm{T}} \in \mathcal{C}^{K\times K}$ embeds the antenna pattern and hardware characteristics, the athmospheric attenuations, the terminals' power and the path losses.

Assuming a transparent feeder link, the values received by the N_{gw} existing gateways can be considered identical to the corresponding entries in $\mathbf{y}_{\mathrm{T}}$. We thus define a splitting in (1) as follows:

$$\begin{pmatrix} \mathbf{y}_1 \\ \mathbf{y}_2 \\ \vdots \\ \mathbf{y}_{N_{\mathrm{gw}}} \end{pmatrix} = \begin{pmatrix} \mathbf{H}_1 \\ \mathbf{H}_2 \\ \vdots \\ \mathbf{H}_{N_{\mathrm{gw}}} \end{pmatrix} \begin{pmatrix} \mathbf{s}_1 \\ \mathbf{s}_2 \\ \vdots \\ \mathbf{s}_{N_{\mathrm{gw}}} \end{pmatrix} + \mathbf{n}_{\mathrm{T}}. \tag{2}$$

Each matrix $\mathbf{H}_n \in \mathcal{C}^{K_n\times K}$ is the short (sometimes called *fat*) matrix representing the channel responses affecting the signals in $\mathbf{y}_n$, the vector which is relayed to the n-th gateway. We will allow each gateway to serve a different number of beams, K_n, as long as the following conditions are met:

$$\sum_{n=1}^{N_{\mathrm{gw}}} K_n = K \qquad K_n \leq \left\lfloor \frac{B_{\mathrm{b}}}{f_{\mathrm{r}} \cdot B_{\mathrm{f}}} \right\rfloor, \quad \forall n. \tag{3}$$

Here, B_{b} denotes the available bandwidth per beam, B_{f} the feeder link bandwidth, and f_{r} the beam frequency reuse factor (reuse one meaning that all the beams share the same frequency band). In consequence, $\lfloor B_{\mathrm{b}}/(f_{\mathrm{r}} \cdot B_{\mathrm{f}}) \rfloor$ denotes the maximum number of beams that a gateway can serve; conversely, the minimum number of required gateways would be given by

$$\min\left[N_{\mathrm{gw}}\right] = \left\lceil \frac{B_{\mathrm{b}} \cdot K}{f_{\mathrm{r}} \cdot B_{\mathrm{f}}} \right\rceil. \tag{4}$$

The channel matrix affecting the signals traveling to each gateway can be further expressed as

$$\mathbf{H}_n = \begin{bmatrix} \tilde{\mathbf{H}}_n & \bar{\mathbf{H}}_{-n} \end{bmatrix} \qquad n = 1, 2, \cdots, N_{\mathrm{gw}} \tag{5}$$

where $\tilde{\mathbf{H}}_n \in \mathcal{C}^{K_n\times K_n}$ comprises the channels from the users served by the n-th gateway, and $\bar{\mathbf{H}}_{-n} \in \mathcal{C}^{K_n\times(K-K_n)}$ the channels of all the other users. Note that each gateway can estimate $\tilde{\mathbf{H}}_n$, but not $\bar{\mathbf{H}}_{-n}$, whose values, if required, must be communicated by the other gateways. If we use $\bar{\mathbf{s}}_{-n}$ to denote the signals managed by all other gateways except n-th, then we rewrite $\mathbf{y}_n$ in (2) for a given gateway as

$$\mathbf{y}_n = \tilde{\mathbf{H}}_n \mathbf{s}_n + \bar{\mathbf{H}}_{-n} \bar{\mathbf{s}}_{-n} + \mathbf{n}_n. \tag{6}$$

III. Multi-gateway LMMSE through sample matrix inversion

In this section, we will explain how to perform interference mitigation separately at each gateway, with the added capability of partial mitigation of the inter-gateway interference. We will focus on linear minimum mean-squared error (LMMSE) combining, since it offers a good trade-off between computational complexity and interference cancellation performance.

Let us start by formulating the LMMSE filter for the n-th gateway. Recall that this is the matrix $\mathbf{W}_n$ such that

$$\mathbf{W}_n = \arg\min_{\mathbf{W}_n} \mathbb{E}\left[\|\mathbf{s}_n - \mathbf{W}_n^H \mathbf{y}_n\|^2\right] \tag{7}$$

which is given by [11]

$$\mathbf{W}_n = \mathbf{R}_{\mathrm{y_n}}^{-1} \mathbf{R}_{\mathrm{y_n s_n}} \tag{8}$$

where

$$\mathbf{R}_{\mathrm{y_n}} \doteq \mathbb{E}\left[\mathbf{y}_n \mathbf{y}_n^H\right] = \mathbf{H}_n \mathbf{H}_n^H + \sigma^2 \mathbf{I}, \tag{9}$$

$$\mathbf{R}_{\mathrm{y_n s_n}} \doteq \mathbb{E}\left[\mathbf{y}_n \mathbf{s}_n^H\right] = \tilde{\mathbf{H}}_n. \tag{10}$$

As explained, we will assume that each gateway has access only to the channel matrix experienced by the users it serves; however, it will not know the full matrix $\mathbf{H}_n$. Thus, in order to compute (8), we propose to use the modified expression

$$\mathbf{W}_n = \hat{\mathbf{R}}_{\mathrm{y_n}}^{-1} \tilde{\mathbf{H}}_n \tag{11}$$

where $\hat{\mathbf{R}}_{\mathrm{y_n}}$ is an estimate of the covariance matrix. Here, for simplicity, we will focus on the sample estimator given by

$$\hat{\mathbf{R}}_{\mathrm{y_n}} = \frac{1}{L} \sum_{\ell=0}^{L-1} \mathbf{y}_{n,\ell} \mathbf{y}_{n,\ell}^H \tag{12}$$

where L is the number of samples used in the estimation, and $\mathbf{y}_{n,\ell}$ denotes the set of signals received at the n-th gateway at time instant ℓ.

This idea has been extensively applied in the field of multi-antenna beamforming, and is usually referred to as sample matrix inversion (SMI) MMSE (see [12] and references therein). Note that, for (11) to work, the number of channel instances averaged, L, has to be greater or equal to K_n for the obtained matrix to be non-singular. Also note that in this way we are able to estimate the full covariance matrix, even though it intrinsically depends on channel coefficients that are not known by the gateway.

We will now expand (12) and write a simplified model for the covariance estimate. Plugging (6) into (12) we obtain

$$\begin{aligned} \hat{\mathbf{R}}_{\mathrm{y_n}} &= \frac{1}{L} \sum_{\ell=0}^{L-1} \left(\mathbf{H}_n \mathbf{s}_{n,\ell} + \mathbf{n}_{n,\ell}\right) \left(\mathbf{s}_{n,\ell}^H \mathbf{H}_n^H + \mathbf{n}_{n,\ell}^H\right) \\ &= \mathbf{H}_n \left(\frac{1}{L} \sum_{\ell=0}^{L-1} \mathbf{s}_{n,\ell} \mathbf{s}_{n,\ell}^H\right) \mathbf{H}_n^H + \frac{1}{L} \sum_{\ell=0}^{L-1} \mathbf{n}_{n,\ell} \mathbf{n}_{n,\ell}^H \\ &\quad + 2\Re\left[\mathbf{H}_n \frac{1}{L} \sum_{\ell=0}^{L-1} \mathbf{s}_{n,\ell} \mathbf{n}_{n,\ell}^H\right]. \end{aligned} \tag{13}$$

In the derivations above, we are assuming that $\mathbf{H}_n$ remains fixed for at least L symbols. However, the potential lack of synchronization among different clusters might cause significant changes in the interfering matrix $\bar{\mathbf{H}}_{-n}$; a close look at this issue would require a detailed system analysis, beyond the scope of this work. In any case, $\hat{\mathbf{R}}_{\mathrm{y_n}}$ needs frequent updates; more detailed considerations on this can be found in Section V.

We will now make a useful simplification; since, for moderately large values of L, it holds that

$$\frac{1}{L} \sum_{\ell=0}^{L-1} \mathbf{s}_{n,\ell} \mathbf{n}_{n,\ell}^H \approx \mathbf{0}, \tag{14}$$

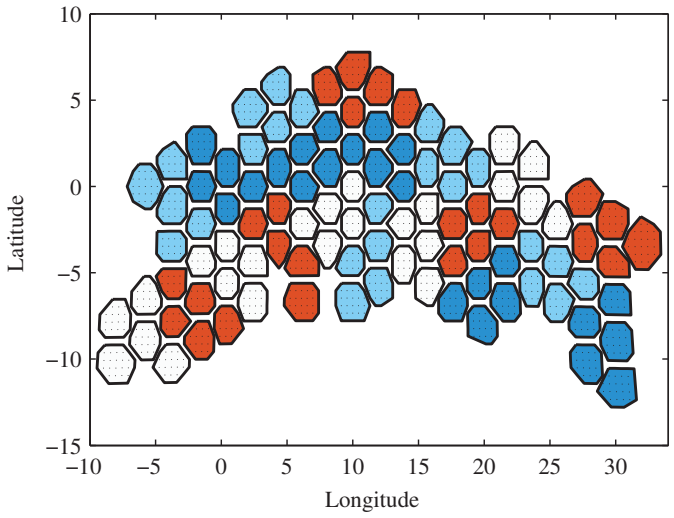

Figure 1. Simulated coverage and clustering pattern used.

then we can rewrite (13) as

$$\begin{aligned}\hat{\mathbf{R}}_{\mathrm{y_n}} &= \mathbf{H}_n \left(\frac{1}{L} \sum_{\ell=0}^{L-1} \mathbf{s}_{n,\ell} \mathbf{s}_{n,\ell}^H \right) \mathbf{H}_n^H + \frac{1}{L} \sum_{\ell=0}^{L-1} \mathbf{n}_{n,\ell} \mathbf{n}_{n,\ell}^H \\ &= \mathbf{H}_n \mathbf{M}_{\mathrm{s}} \mathbf{H}_n^H + \mathbf{M}_{\mathrm{n}}\end{aligned} \tag{15}$$

where we have defined $\mathbf{M}_{\mathrm{s}} \doteq 1/L \cdot \sum_{\ell=0}^{L-1} \mathbf{s}_{n,\ell} \mathbf{s}_{n,\ell}^H$. It is easy to check that $\mathbf{M}_{\mathrm{n}}$ is a complex Wishart matrix [13], $\mathbf{M}_{\mathrm{n}} \sim \mathcal{CW}_{K_n}(L, \sigma^2 \mathbf{I})$, very easy to generate for simulation purposes; note that the same result does not apply for $\mathbf{M}_{\mathrm{s}}$, since the elements in $\mathbf{s}_{\mathrm{n}}$ are dragged from the set of symbols in the constellation, $\mathcal{S}$.

It shall be remarked that, at the cost of some additional computational complexity, more accurate estimators for $\mathbf{R}_{\mathrm{y_n}}$ could be formulated, since a partial knowledge of the elements in $\mathbf{R}_{\mathrm{y_n}}$ is available by considering $\tilde{\mathbf{H}}_n$ known. We will not explore this further throughout this paper since, as we will show in the next section, the accuracy of the estimator is not the performance bottleneck.

IV. Simulation results

A. Scenario description

Let us describe the simulated scenario, which is very similar to the one used in [14], in the context of the SatNEx III project [15].

We simulated the return link of a multibeam satellite coverage operating at 30 GHz (Ka-band), with full frequency reuse, and based on the DVB-RCS2 standard [16]. One hundred beams are served through an antenna with the same number of radiating elements, and whose pattern was provided numerically. We assume a transparent feeder link with an available bandwidth of 2.5 GHz, and a user link bandwidth equal to 500 MHz. As a result, the processing has to be split among 20 clusters, and thus $N_{\mathrm{gw}} = 20$ and $K_n = 5$ for all n; the beam coverage and the clustering adopted for the simulations can be seen on Figure 1. The total receiver noise temperature is 517 K. The baudrate is 4 Msymb/s and the guardbands amount to 11% of the carrier bandwidth, with a filter rolloff factor of 0.25. As baseline case without multiuser detection, we consider a frequency reuse factor of three, with 166 MHz per beam. For illustration purposes, simulation results cover a large range of transmit powers, although it is important to stress that the most extreme values do not correspond to practical cases.

Table I
DVB-RCS2 Modulation and Coding Schemes (MCS) Description.

MCS	η (bps/Hz)	Req. SNR (dB)
QPSK_13	0.53	−0.45
QSPK_12	0.8	1.80
QPSK_23	1.07	3.75
QPSK_34	1.2	4.85
QPSK_56	1.33	6.10
8PSK_23	1.6	7.60
8PSK_34	1.8	8.90
8PSK_56	2	10.30
16QAM_34	2.4	11.20
16QAM_56	2.67	12.20

Results have been averaged for 10^4 channel realizations for each EIRP point. The randomness of the channel is due to the position of the users, which are assumed to be uniformly distributed within each spot, and to the rain attenuation, which we assume independently distributed among the beams; the statistical parameters of such attenuation are assumed to be the same in every beam, and represented by an empirical distribution as in [14].

For each realization, the SINR for each user is computed for the baseline scenario (frequency reuse three and no multiuser detection), for the single gateway LMMSE receiver with perfect channel knowledge, and for the per-gateway LMMSE filtering with estimated covariance matrix. Covariance estimation is computed following (15). For a more realistic performance assessment, throughput and outage figures are obtained from the SINR according to the specifications of DVB-RCS2 (see Table I). More precisely, let T_{ij} be the corresponding throughput achieved by mapping the SINR values into the DVB-RCS2 specifications, for the i-th channel realization in the j-th beam. Then we define the total throughput as

$$\mathrm{total\_throughtput} = \sum_{j=1}^{100} \frac{\sum_{i=1}^{N_{\mathrm{sims}}} T_{ij}}{\sum_{i=1}^{N_{\mathrm{sims}}} \mathcal{I}\left[T_{ij}\right]} \tag{16}$$

where $\mathcal{I}[x]$ is the indicator function, which takes the value 1 if x is non-zero, and 0 otherwise. Note that $1/\sum_{i=1}^{N_{\mathrm{sims}}} \mathcal{I}\left[T_{ij}\right]$ represents the time fraction that the j-th beam corresponding user gets some useful rate. By defining the throughput this way, we are only accounting for the active users, whereas those suffering from high interference levels which cannot be compensated by the proposed mitigation mechanism are

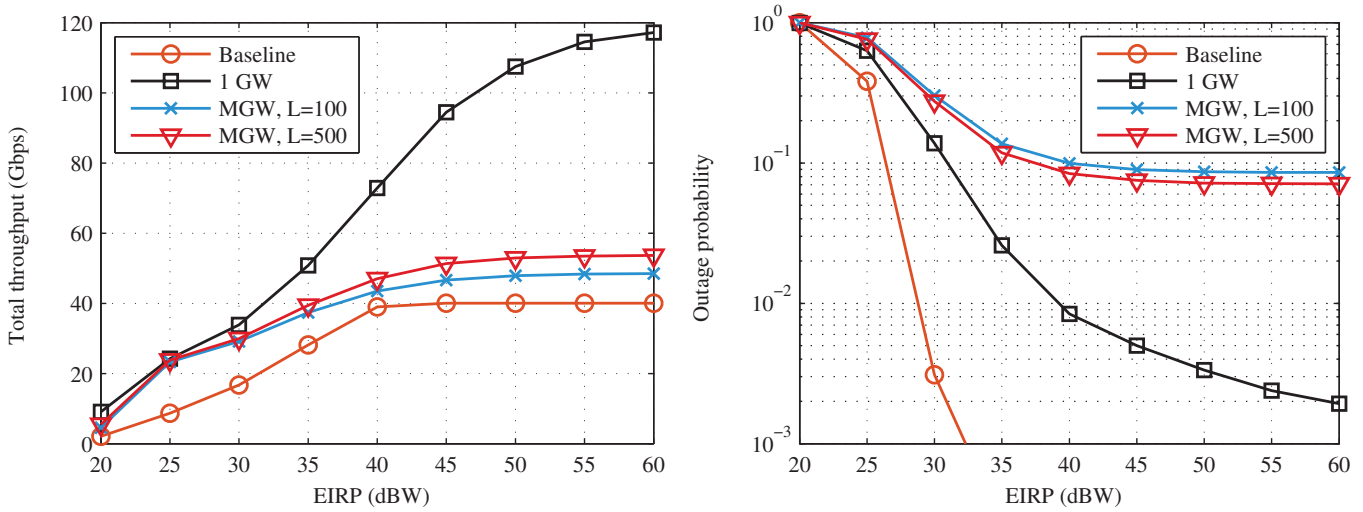

Figure 2. Throughput (left) and outage probability (right) for the baseline scenario, and different types of multi-gateway MUD.

declared as unavailable or in outage. In this regard, the outage probability is computed as

$$\text{outage\_probability} = 1 - \frac{1}{100 \cdot N_{\text{sims}}} \sum_{j=1}^{100} \sum_{i=1}^{N_{\text{sims}}} \mathcal{I}\left[T_{ij}\right]. \tag{17}$$

B. Results

Throughout this section, the term *baseline* refers to frequency reuse three and no multiuser detection; the tag *1 GW* refers to the ideal case with a single gateway, perfect knowledge of the covariance matrix, and LMMSE processing; the tag *MGW* refers to the case with multiple gateways, LMMSE processing, and the covariance matrix estimated with L time samples.

Figure 2 shows the performance of different techniques in terms of throughput (left) and outage (right). We can see that multi-gateway processing with no cooperation and covariance estimation still improves the throughput of the baseline scenario in a noticeable way. However, outage probability suffers a drastic increase, and it soon experiences a horizontal asymptote. This is because of the residual interference present in the multi-gateway case, which cannot be removed. For a more detailed assessment of the throughput behavior, Figure 3 zooms in the region between EIRP $= 40$ dBW and EIRP $= 50$ dWB. We can see that, at EIRP $= 45$ dBW, the throughput with multiple gateways and $L = 500$ increments a 28% with respect to baseline; with a single gateway, the performance could have been improved up to a 136%. In this plot we have also added a curve tagged *MGW partial*, which shows the results obtained with LMMSE and the covariance matrix built as $\hat{\mathbf{R}}_{\text{y}_\text{n}} = \tilde{\mathbf{H}}_n \tilde{\mathbf{H}}_n^H + \sigma^2 \mathbf{I}$, that is, built from the perfect knowledge of $\tilde{\mathbf{H}}_n$ but without considering the inter-gateway terms[2]. Throughput decreases with respect to the

[2]Note that the noise variance needs to be known for the implementation of this alternative approach.

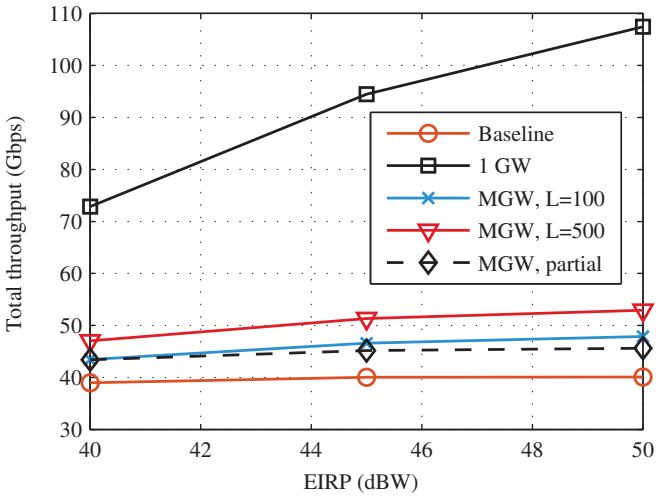

Figure 3. Zoom in the throughput behavior.

blind estimation of $\mathbf{R}_{\text{y}_\text{n}}$, in what can be considered as an additional evidence of the importance of accounting for inter-gateway interference. For further insights, Figure 4 shows the complementary cumulative distribution of the output SINR for each technique discussed. It can be seen the degradation in the SINR due to the uncancelled interference for all full-frequency reuse versions. Nevertheless, the three-fold bandwidth increase keeps the advantage in terms of achieved throughput.

C. Covariance estimation requirements

As explained, there are many available results in the literature regarding the covariance matrix estimation, and some additional accuracy might be expected by exploiting our knowledge of its structure. However, in our simulations we noticed that further increments in L did not improve the performance, as $L = 500$ already provides a very accurate

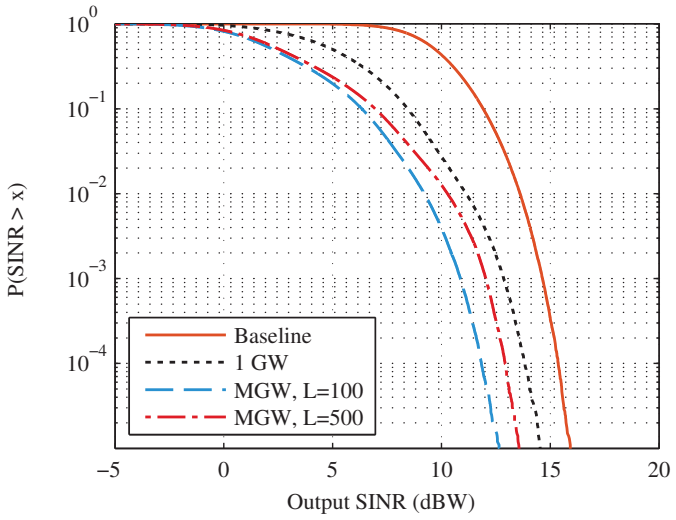

Figure 4. CCDF of the output SINR of the different techniques.

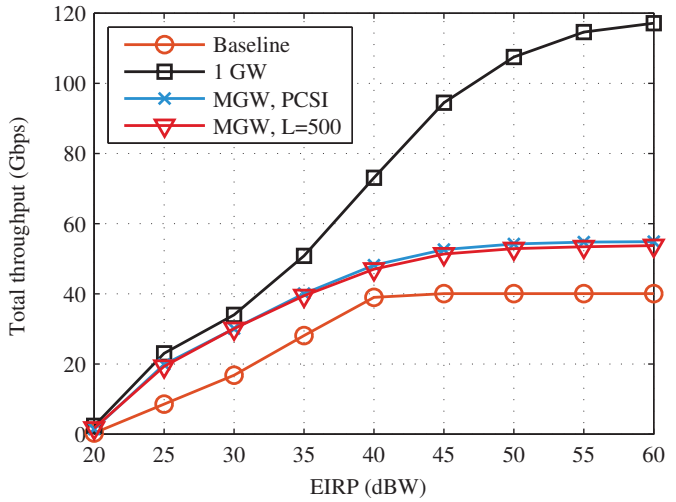

Figure 5. Throughput for different techniques.

estimation. This can be seen in Figure 5, where the tag *MGW PCSI* denotes the multi-gateway cancellation strategy with perfect knowledge of the covariance matrix $\mathbf{R}_{\mathrm{y_n}}$. As we can see, there are minimal differences between its throughput and that with $L = 500$.

V. Practical considerations

A. Estimate updating

Throughout the paper, we have been performing an estimation of the covariance matrix, with L samples, for each time instance of the channel matrix $\mathbf{H}_n$. The maximum number of L is limited by the time coherence of the channel. For fixed satellite scenarios as that in Section IV, the channel coherence is in the order of hundreds of seconds [17], while typical symbol periods are in the order of tens of microseconds. In consequence, the evolution of $\mathbf{H}_n$ will be rather conditioned by the interference term $\bar{\mathbf{H}}_{-n}$ in (5), which is expected to change faster due to the probable lack of synchronism among different gateways. Updating of the estimate $\hat{\mathbf{R}}_{\mathrm{y_n}}$ to follow the evolution of the channel can be implemented by means of the recursive least-squares (RLS) estimation [18]. Initially, we build the first estimate as $\sum_{\ell=0}^{L-1} \mathbf{y}_\ell \mathbf{y}_\ell^H$, with $L \geq K_n$ so that the resulting matrix can be inverted. Note that we are dropping the gateway index n for simplicity. Then, we update the estimate after the reception of a new set of samples $\mathbf{y}$,

$$\hat{\mathbf{R}}_{\mathrm{y}}^{\ell} = \lambda \hat{\mathbf{R}}_{\mathrm{y}}^{\ell-1} + \mathbf{y}_\ell \mathbf{y}_\ell^H \qquad 0 < \lambda < 1 \tag{18}$$

where λ denotes the forgetting factor. Now, direct inversion of the new $K_n \times K_n$ covariance estimate is not needed; since we are just performing a rank-one update in each step, we can use the RLS algorithm and write

$$\left(\mathbf{R}_{\mathrm{y}}^{\ell} + \frac{1-\lambda}{\lambda}\mathbf{y}_\ell \mathbf{y}_\ell^H\right)^{-1} = \left(\mathbf{R}_{\mathrm{y}}^{\ell}\right)^{-1} - \frac{\alpha}{1 + \alpha \mathbf{y}_\ell^H \left(\mathbf{R}_{\mathrm{y}}^{\ell}\right)^{-1} \mathbf{y}_\ell} \left(\mathbf{R}_{\mathrm{y}}^{\ell}\right)^{-1} \mathbf{y}_\ell \mathbf{y}_\ell^H \left(\mathbf{R}_{\mathrm{y}}^{\ell}\right)^{-1} \tag{19}$$

which is a direct application of Woodbury's identity [19], and where $\alpha = (1-\lambda)/\lambda$.

B. Estimation of $\tilde{\mathbf{H}}_n$

In our simulations, we assumed that each gateway had perfect knowledge of the coefficients of its served beams, $\tilde{\mathbf{H}}_n$. In practice, such a knowledge will never be perfect, and $\tilde{\mathbf{H}}_n$ entries will be acquired through pilot sequences and, for example, least squares estimation. Some degradation in performance is expected due to non-perfect channel estimation; this degradation would decrease for larger pilot sequences.

C. Cluster definition and gateway placement

The performance, specially in terms of outage, is still limited for the multi-gateway processing scenario due to the residual interference. The way clusters are defined is crucial to this end. In this work we have used an *ad hoc* grouping based on proximity on the plane, but more elaborate clusterings could be possible, keeping in mind that gateways should not be placed close to each other in angular separation.

VI. Conclusions

In this paper, we have tested the use of inter-gateway interference mitigation in a multibeam satellite return link in the absence of collaboration among the gateways. This is achieved by blindly estimating the covariance matrix of the useful signal plus noise and interference at each gateway, and then applying LMMSE combining. With respect to a three-colors baseline scenario, results have shown a noticeable throughput increase when link is available. The loss in availability is especially harmful for those users suffering from high interference levels which cannot be compensated by the blind mitigation scheme. It was also shown that estimating the covariance matrix with 500 samples clearly improves the results of using only the channels available to the gateway, and already performs

close to the ideal covariance knowledge case. In order to improve the availability results, further investigation is needed, possibly through the exchange of some information across the gateways.

Table II
SUMMARY OF THE OBTAINED RESULTS, EIRP $= 45\,\mathrm{dBW}$.

	Throughput (Gbps)	Outage probability
Baseline	40	$< 10^{-4}$
MGW, $L = 500$	~~41.32~~ (+28%)	$7 \cdot 10^{-2}$
1 GW	94.47 (+136%)	$3 \cdot 10^{-3}$

REFERENCES

[1] Cisco Systems, "Cisco visual networking index: Global mobile data traffic forecast update, 2013–2018," Tech. Rep., 2014.

[2] N. Letzepis and A. Grant, "Capacity of the multiple spot beam satellite channel with Rician fading," *IEEE Trans. Inf. Theory*, vol. 54, no. 11, pp. 5210 –5222, Nov. 2008.

[3] J. Arnau, D. Christopoulos, S. Chatzinotas, C. Mosquera, and B. Ottersten, "Performance of the multibeam satellite return link with correlated rain attenuation," *IEEE Trans. Wireless Commun.*, vol. 13, no. 11, pp. 6286 – 6299, Nov. 2014.

[4] M. Debbah, G. Gallinaro, R. Müller, R. Rinaldo, and A. Vernucci, "Interference mitigation for the reverse-link of interactive satellite networks," in *Proc. SPSC*, Noordwijk, The Netherlands, Sep. 2006.

[5] A. Panagopoulos, P. D. M. Arapoglou, and P. Cottis, "Satellite communications at Ku, Ka, and V bands: Propagation impairments and mitigation techniques," *IEEE Commun. Surveys Tuts.*, vol. 6, no. 3, pp. 2–14, 2004.

[6] A. Kyrgiazos, B. Evans, and P. Thompson, "On the gateway diversity for high throughput broadband satellite systems," *IEEE Trans. Wireless Commun.*, vol. 13, no. 10, pp. 5411–5426, Oct. 2014.

[7] C. Kourogiorgas, A. Panagopoulos, and J. Kanellopoulos, "On the Earth-space site diversity modeling: novel physical-mathematical outage prediction model," *IEEE Trans. Antennas Propag.*, vol. 60, no. 9, pp. 4391–4397, Sep. 2012.

[8] L. Cottatellucci, M. Debbah, G. Gallinaro, R. Mueller, M. Neri, and R. Rinaldo, "Interference mitigation techniques for broadband satellite systems," in *Proc. ICSSC*, Naples, Italy, Oct. 2006.

[9] G. Zheng, S. Chatzinotas, and B. Ottersten, "Multi-gateway cooperation in multibeam satellite systems," in *Proc. PIMRC*, Sydney, Australia, 2012, pp. 1360–1364.

[10] F. Lombardo, A. Vanelli-Coralli, E. Candreva, and G. Corazza, "Multi-gateway interference cancellation techniques for the return link of multi-beam broadband satellite systems," in *Proc. IEEE GLOBECOM*, Anaheim, CA, Dec. 2012, pp. 3425–3430.

[11] S. M. Kay, *Fundamentals of statistical signal processing: estimation theory*. Upper Saddle River, NJ, USA: Prentice-Hall, Inc., 1993.

[12] X. Mestre and M. Lagunas, "Finite sample size effect on minimum variance beamformers: optimum diagonal loading factor for large arrays," *IEEE Trans. Signal Process.*, vol. 54, no. 1, pp. 69–82, Jan. 2006.

[13] R. Couillet and M. Debbah, *Random Matrix Methods for Wireless Communications*. Cambridge University Press, 2011.

[14] J. Arnau, B. Devillers, C. Mosquera, and A. Perez-Neira, "Performance study of multiuser interference mitigation schemes for hybrid broadband multibeam satellite architectures," *EURASIP J. Wirel. Commun. Netw.*, p. 132, 2012.

[15] "The SatNEx III project." [Online]. Available: http://www.satnex.org/

[16] ETSI EN 301 545-2, "Digital Video Broadcasting (DVB); Second Generation DVB Interactive Satellite System; Part 2: Lower Layers for Satellite standard," 2011.

[17] B. Gremont and M. Filip, "Spatio-temporal rain attenuation model for application to fade mitigation techniques," *IEEE Trans. Antennas Propag.*, vol. 52, no. 5, pp. 1245 – 1256, May 2004.

[18] S. Haykin, *Adaptive filter theory*. Prentice Hall, 2002.

[19] R. Horn and C. Johnson, *Matrix Analysis*. Cambridge University Press, 1990.